Probabilistic Seismic Loss Analysis for the Design of Steel Structures: Optimizing for Multiple-Objective Functions

Sanaz Saadat,[a)] M.EERI, **Charles V. Camp**[b)] **and Shahram Pezeshk,**[b)] M.EERI

An optimized seismic performance-based design (PBD) methodology considering structural and nonstructural system performance and seismic losses is considered to optimize the design of a steel structure. Optimization objectives are to minimize the initial construction cost associated with the weight of the structural system and the expected annual loss (EAL), considering direct economic losses. A non-dominated sorting genetic algorithm method is implemented for the multi-objective optimization. Achieving the desired confidence levels in meeting performance objectives of interest are set as constraints of the optimization problem. Inelastic time history analysis is used to evaluate structural response under different levels of earthquake hazard to obtain engineering demand parameters. Hazus fragility functions are employed for obtaining the damage probabilities for the structural system and nonstructural components. The optimized designs and losses are compared for the structure located in two geographic locations: one in the central United States and another in the western United States. [DOI: 10.1193/080513EQS223M]

INTRODUCTION

Civil structures are typically designed, based on their location and type, to withstand different types of hazards such as earthquakes, wind, etc. Performance-based design (PBD) is an alternative to traditional design procedures, which are generally force-based design methods (Bazeos 2009) and provide requirements for life safety protection (Hamburger et al. 2004) but lack detailed expressions for levels of earthquake-induced damage. PBD pursues meeting the performance objectives, which are defined as meeting specified performance levels (such as immediate occupancy or collapse prevention) for certain hazard levels. In addition, PBD can provide more understanding regarding the performance of a structure to probable hazards. The performance objectives are based on the safety and economy of a structure. In seismic PBD, performance objectives should be met for earthquake ground motions related to different hazard levels. The uniqueness and advantage of the PBD is that it uses a probabilistic approach in evaluating the performance of a structure in meeting performance objectives (Augusti and Ciampoli 2008). In the first generation of PBD procedures, performance concepts are introduced in terms of discretely defined performance levels that are linked to specific hazard levels (FEMA 2006). From a probabilistic view,

[a)] 104 Eng. Science Bldg, Dept. of Civil Eng., University of Memphis, TN 38152
[b)] 104 Eng. Science Bldg, Dept. of Civil Eng., University of Memphis, TN 38152

estimating a building's performance and characteristics during future earthquake events is considered by introducing confidence levels in meeting performance objectives. In addition, in recent recommended frameworks for the next-generation PBD, the probable performance of structures in future earthquakes would be expressed in quantitative statements of the risk of casualty, occupancy and economic losses (Hamburger et al. 2004, FEMA 2006).

Seismic risk assessment is an important part of real estate financial decision making for regions at risk of damaging earthquakes (ASTM 2007). Estimating the variability of earthquake risk would be very useful for developing mitigation policies and planning funding levels in both the public and private sectors. Applying seismic design codes and using specialized construction techniques might reduce potential losses in new buildings; however, the economics evaluation of these solutions requires evidence of risk (FEMA 2008). Expected annual loss (EAL) is a common term in earthquake loss estimation and an outcome of seismic risk assessment that measures the average yearly loss which accounts for frequency and severity of various levels of loss (Porter et al. 2004).

Different objectives can be used to optimize the PBD of structures. Beck et al. (2000) introduced an optimal PBD methodology by incorporating multiple preference functions and aggregating them using multiplicative trade-off strategy. Ganzerli et al. (2000) minimized the structural cost subjected to performance constraints on plastic rotations of beams and columns and behavioral constraints for reinforced concrete frames. Liu et al. (2005) formulated the seismic performance-based design of steel moment frames as multi-objective optimization problem considering present capital investment and future seismic risk which is considered in terms of maximum interstory drift demands at two hazard levels. Xu et al. (2006) presented a multi-criteria optimization for seismic PBD of steel structures under equivalent static seismic loading that minimized cost and earthquake damage. Fragiadakis et al. (2006) performed a performance-based optimum design of steel structures considering life cycle cost. Alimoradi et al. (2007) and Foley et al. (2007) used a multi-objective optimization in the performance-based design of steel structures in which their objectives were the weight of the structure and a confidence parameter calculated based on the procedure presented in FEMA (2000a). Genturk and Elnashai (2011) considered reducing the life-cycle cost of buildings by reductions in material usage and seismic damage cost to achieve the objectives of economy and sustainability. Rojas et al. (2011) developed a multi-objective optimization PBD of steel structures using the weight of the structure and the expected annual loss as the optimization objectives.

In this study, seismic loss evaluations are considered in optimizing the PBD of steel structures. Probabilistic hazard analysis is used to measure the potential losses due to earthquake in two different sites; Memphis, Tennessee, located in the central United States (CUS) and Los Angeles, California, located in the western United States (WUS). A multi-objective optimization is implemented to minimize the combination of the initial construction cost, which is modeled by the weight of the structural system, and EAL associated with direct economic losses. Inelastic time history analysis is used to evaluate structural response under different levels of earthquake hazard to obtain engineering demand parameters considered as inter-story drifts and peak floor accelerations. The calculated EAL provides planners and engineers with a risk-based method for evaluating alternative structural designs and a quantitative parameter to compare seismic risks in different geographic locations.

OPTIMIZATION PROBLEM

The multi-objective optimization attempts to minimize the combination of the initial cost associated with the weight of the structural system (w) and EAL of a building while achieving the desired confidence levels for performance objectives and seismic design codes. The performance objectives are immediate occupancy performance level for the hazard level of 50% probability of exceedance (POE) in 50 years and collapse prevention for the hazard level of 2% POE in 50 years. This optimization problem can be rather computationally expensive, since it requires the inelastic time history analysis for a large number of ground motions to perform the loss analysis. The general form of the optimization statement is defined as:

$$Minimize(W, L) \quad Subjected\ to\colon c_i \ (i = 1, 4) \tag{1}$$

where W and L are the penalized values for the weight (w) and EAL of the structure, respectively; and c_i is the i^{th} constraint that is applied on the optimization problem. The penalized values W and L are calculated as:

$$W = \varphi \times w \tag{2}$$

$$L = \varphi \times EAL \tag{3}$$

where φ is the penalty function. The constraints for the confidence levels for collapse prevention CL_{CP} and immediate occupancy CL_{IO} are:

$$c_1\colon \frac{CL_{CP}}{CL_{CP,\min}} \geq 1.0 \tag{4}$$

$$c_2\colon \frac{CL_{IO}}{CL_{IO,\min}} \geq 1.0 \tag{5}$$

where $CL_{CP,\min} = 90\%$ and $CL_{IO,\min} = 50\%$, as recommended by FEMA 350 (FEMA 2000a). Calculation of CL values is based on FEMA 350 recommendations and is further explained in the following sections (Equations 14 to 16). The constraint for ensuring the AISC strong column-weak beam criteria of for seismic design, calculated for each connection in the frame is:

$$c_3\colon \frac{\sum M_{pc}^*}{\sum M_{pb}^*} \geq 1.0 \tag{6}$$

where M_{pc}^* is the modified flexural strength of the column and M_{pb}^* is the modified flexural strength of beam sections (neglecting the additional moment due to shear amplification from the location of the plastic hinge to the column centerline). Equation 6 is calculated using the AISC (2011) specifications section E3. The constraint for flexural capacities to be greater than the flexural demands due to gravity loads is:

$$c_4\colon \frac{C_e}{D_g} \geq 1.0 \tag{7}$$

where C_e is the flexural capacity of the frame elements, calculated based on AISC (2011) recommendations for the of capacity of elements in flexure, and D_g is the flexural demand for the structure subjected to only gravity loads.

Penalty function, φ, is defined as:

$$\phi = \prod_{i=1}^{4} \phi_i \quad where \begin{cases} \phi_i = 2.0 - c_i & if\ c_i < 1.0 \\ \phi_i = 1.0 & if\ c_i \geq 1.0 \end{cases} \tag{8}$$

A multi-objective genetic algorithm (GA) using an elitist non-dominated sorting strategy, NSGA-II (Deb et al. 2002), is implemented to perform the optimization. A GA is a stochastic optimization method that attempts to mimic the process of natural selection. In a GA, a fitness value is computed for individual members in the population based on the optimization objective and the population is evolved over many generations by means of GA operators (i.e., selection, crossover, mutation, etc.). Individuals within the population with better fitness values have a higher chance of being selected and survival through the process. In multi-objective optimization, since there are several objectives being optimized simultaneously, there is not a single solution that would be optimal for all objectives. Instead, there is a set of non-dominated solutions, known as Pareto optimal solutions (Gen and Cheng 2000). In order to preserve the diversity of the solutions in the Pareto front (set of Pareto-optimal solutions), a crowding distance methodology is used. The first step in this optimization strategy is to randomly generate a population and compute a fitness value for each parent individual in the population based on a non-dominated sorting. Fitness is assigned to individuals based on the number of solutions they dominate (i.e., number of solutions that they excel in both objectives). A new child population is generated based on general GA methodology (roulette wheel selection, uniform crossover, and mutation). Next, a new population is developed from the parent and child populations by grouping individuals into subsets of different fronts based on the non-dominated sorting procedure. The next generation is populated with members for the first front. If the new generation is not fully populated from the first front pool, members are taken form the second front, and so on, until the new generation is fully populated. If there are fewer unfilled positions in the new generation than there are members in a front group, a crowding distance sorting strategy is applied where individuals with larger crowding distances are chosen to fill out the parent population.

LOSS CALCULATION

Seismic performance and loss estimation of a structure can be organized into four steps: (1) probabilistic seismic hazard analysis (PSHA); (2) probabilistic seismic demand analysis (structural analysis); (3) probabilistic capacity analysis (fragility analysis or damage analysis); and (4) probabilistic loss analysis (Porter 2003, Bachman 2004, Deierlein 2004, Miranda et al. 2004, Moehle and Deierlein 2004, and Krawinkler 2005). The results of all these steps are aggregated using the total probability theorem. Pacific Earthquake Engineering Research (PEER) has proposed a loss assessment framework to calculate the mean annual occurrence rate of decision variable $\lambda[DV]$ (Moehle and Deierlein 2004, Krawinkler 2005, Ramirez et al. 2012) as:

$$\lambda[DV] = \iiint P[DV|DM]P[DM|EDP]P[EDP|IM]\lambda[IM]dDMdEDPdIM \tag{9}$$

where DV is the decision variable, DM is the damage measure, EDP is the engineering demand parameter, and IM is the intensity measure. The cumulative distribution function of the random variable X conditioned on random variable Y is $P[X|Y]$.

PROBABILISTIC SEISMIC HAZARD ANALYSIS (PSHA)

The first step in seismic performance analysis for a structure is to have suits of ground motion compatible with different hazard levels that should be used to evaluate the performance of the structure for various performance objectives. The goal of PSHA is to quantify the uncertainties regarding the location, size, and resulting shaking intensity of a possible future earthquake at a given site and combine the results to produce an explicit description of the distribution of future shaking in that site (Baker 2008). For a structure located in Memphis, EZ-FRISK (Risk Engineering, Inc.) is used to perform PSHA. The New Madrid seismic zone (NMSZ) and CUS gridded data are considered as seismic sources and the attenuation relationships recommended by USGS (2008) are implemented. EZ-FRISK generates the uniform hazard response spectra (UHRS) for different hazard levels. Figure 1 shows the obtained response spectra for hazard levels considered for Memphis, with 2%, 5%, 10%, and 50% POE in 50 years.

Due to the scarcity of the strong ground motion recorded data available in the NMSZ, the computer program SMSIM (Boore 2000) is used to generate synthetic time histories for Memphis. In order to have ground motions that are compatible with UHRS at each hazard level, the spectral matching procedure presented by Shahbazian and Pezeshk (2010) is used.

Site amplification effects are considered by using the SHAKE91 computer program. Properties for a site located in Memphis are selected based on the information given by Romero and Rix (2001) for Lowlands geological conditions. Damping and modulus degradation curves are adopted from EPRI (1993).

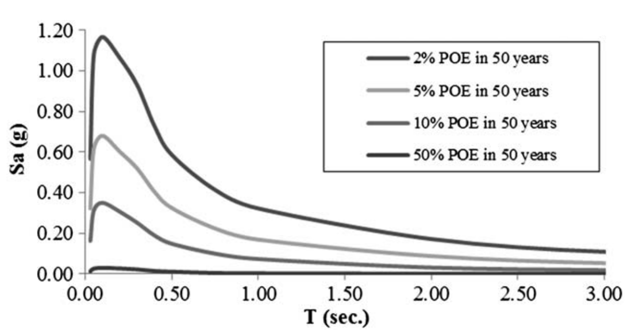

Figure 1. Spectral accelerations for different hazard levels for a site located in Memphis obtained from EZ-FRISK.

For a site located in Los Angeles, suites of ground motions for three different hazard levels, 2%, 10%, and 50% POE in 50 years, are from the SAC steel research project (Somerville et al. 1997). The ground motions are scaled so that, on average, their spectral values match with a least square error fit to the USGS mapped values at 0.3 s, 1.0 s, and 2.0 s, and an additional predicted value at 4.0 s (Somerville et al. 1997). The weights assigned to the four period points are 0.1 at the 0.3 s period point and 0.3 for the other three period points. The target spectra provided by USGS are for the S_B/S_C soil type boundaries, which have been modified to be representative for soil type S_D (FEMA 2000b).

PROBABILISTIC SEISMIC DEMAND ANALYSIS

The second step in the loss assessment process of a structure is to determine the appropriate engineering demand parameters (EDPs) to best describe its response (Bachman 2004). The EDPs (e.g., inter-story drifts, column compressive forces, etc.) are obtained from analyses of a structure for ground motions at different hazard levels. Nonlinear time-history analysis using the DRAIN-2DX computer program (Prakash et al. 1993) is used to obtain the EDPs. Inter-story drift (ISD) and peak floor acceleration (PFA) are considered as EDPs for calculation of the direct economic loss of the building. Yield surfaces for the structural elements are based on the models presented in Powell (1993), Alimoradi (2004), and Rojas et al. (2011).

PROBABILISTIC CAPACITY ANALYSIS

The EDPs for structural and nonstructural components are linked to damage measures (*DM*s) which describe the physical condition of these components. For the purpose of damage assessment, fragility curves for the structure of interest should be developed. Fragility functions are probability distributions to indicate the likelihood of damage to an element or system due to a given damage state as a function of a single demand parameter such as the ISD or the PFA (ATC 2007). Fragility curves are defined as lognormal distribution of the conditional probability of damage exceeding certain *DM* given *EDP* (Hazus-MH 2003a and Rojas 2008) which can be expressed as:

$$P[DM|EDP] = \Phi\left[\frac{1}{\beta_{DM}} \ln \frac{EDP}{EDP_{DM}}\right] \tag{10}$$

where EDP_{DM} is the median value of the considered *EDP* (e.g., ISD) and β_{DM} is the lognormal standard deviation of the *EDP* for the *DM* considered (such as slight, moderate, extensive, and complete).

Fragility curves are obtained using the parameters given for generic fragility functions in Hazus technical manual Hazus-MH (2003a) for structural and nonstructural members for different damage states. It should be noted that generic fragility functions have been implemented to simplify the procedure, which would result in having less accurate result, as compared to implementing building specific fragility functions. Authors have not compared the results with other methods that employ these functions. Building specific fragility curves could be updated and improved for the future studies. Figures 2 through 4 show the fragility curves for a low-rise building type S1 (steel moment frames) with high-code seismic design level. Values of β_{DM} are determined from Hazus-MH (2003a). Figure 5 shows an example of

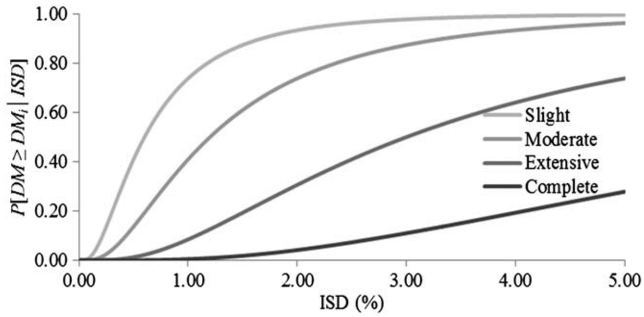

Figure 2. Fragility curves for structural (SS) elements for sample structure.

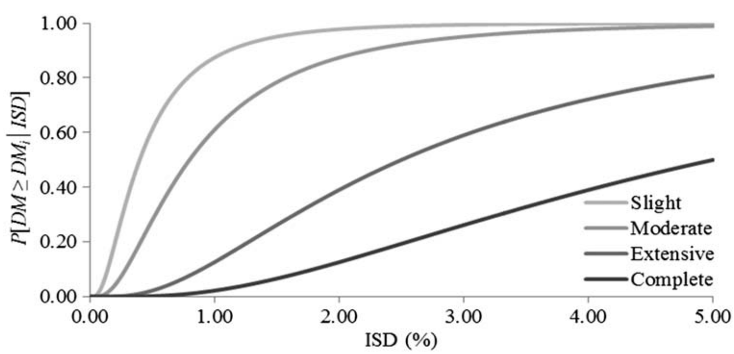

Figure 3. Fragility curves for drift-sensitive nonstructural (NSD) elements for sample structure.

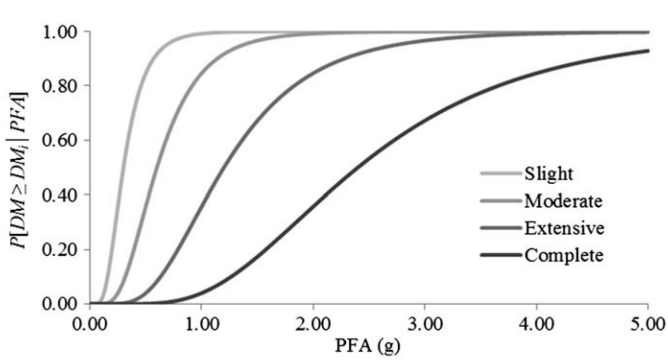

Figure 4. Fragility curves for acceleration-sensitive nonstructural (NSA) elements for sample structure.

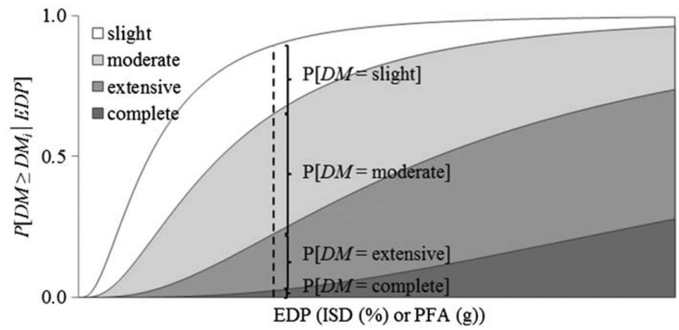

Figure 5. Damage analysis for different components.

damage analysis. This analysis would be performed for structural components (SS), drift sensitive (NSD), and acceleration sensitive (NSA) nonstructural components.

PROBABILISTIC LOSS ANALYSIS

The final step in the loss calculation is the calculation of the *DV*s that serve to translate damage estimates into quantities that are useful for risk-related decisions. The *DV*s relate to one or more of the three metrics: direct dollar losses, downtime (or restoration time), and deaths (casualties). In this study, the *DV* is the direct economic loss, expressed in percent of building replacement cost (%BRC). Table 1 lists the repair cost (RC) ratios (%BRC) for different components and different damage measures for a building with a commercial COM4 occupancy class (Hazus-MH 2003b). According to the Hazus manual, the structural components include the costs associated with the structural system of the building. Acceleration sensitive nonstructural components include: hung ceilings, mechanical and electrical equipment, and elevators. Drift-sensitive components include: partitions, exterior wall panels, and glazing.

The methodology for calculation of EAL associated with direct economic losses, explained by Equations 11 to 13, is similar to those given by ATC (2007), Rojas (2008), and Hazus-MH (2003b). Expected economic losses $E[L_{c,EDP}]$ (%BRC) for each component (SS, NSD, NSA), are calculated for a specific *IM* as:

Table 1. Considered RC ratios (%BRC) for different components and different damage measures (Hazus-MH 2003b)

	RC (%BRC)			
Component	Slight	Moderate	Extensive	Complete
SS	0.4	1.9	9.6	19.2
NSD	0.9	4.8	14.4	47.9
NSA	0.7	3.3	16.4	32.9

$$E[L_{c,EDP}] = \sum_{i=2}^{5} P[DM_{i,EDP}] \times RC_{DMi,c} \tag{11}$$

where $L_{c,EDP}$ is the loss associated with each component c (SS, NSD, and NSA) for the EDP at a specific IM, $P[DM_{i,EDP}]$ is calculated using fragility curves for the EDP at a specific IM, and $RC_{DMi,c}$ is defined as the repair cost for each component due to DM_i which varies from slight ($i = 2$) to complete ($i = 5$; Hazus-MH 2003b). Expected loss $E[L_{EDP}]$ for a particular structure is calculated as the sum of losses for all components as:

$$E[L_{EDP}] = E[L_{SS,EDP}] + E[L_{NSD,EDP}] + E[L_{NSA,EDP}] \tag{12}$$

The expected loss E$[L_{EDP}]$ is calculated for different intensity measures. For example, for a site located in Memphis, having ten time histories for four hazard levels requires the calculation of loss values for 40 ground motion time histories for each individual structure. The resulting loss curves are developed from a cumulative distribution of losses for each hazard level (ATC 2007 and Rojas et al. 2011).

Figures 6 and 7 show the distribution of losses for different hazard levels for Memphis and Los Angeles, respectively, for a sample structure. RC_T is the total repair cost of the structure presented in percent of building replacement cost (BRC).

The next step is the aggregation of losses from different hazard levels. For Memphis, the hazard curve is obtained from EZ-FRISK. Figures 8 and 9 show the implemented hazard curves for Memphis and Los Angeles, respectively. The hazard curves are obtained by amplifying values for bedrock by factors for site class D presented in AASHTO (2009). The total loss curve is obtained from loss curves for each hazard level and hazard curve as (ATC 2007, FEMA 2012):

$$P[L > l]/yr = \int_{\lambda} P[L > l|IM]d\lambda \approx \sum_{i=1}^{m} (1 - P[L < l|IM_i])\Delta\lambda_i \tag{13}$$

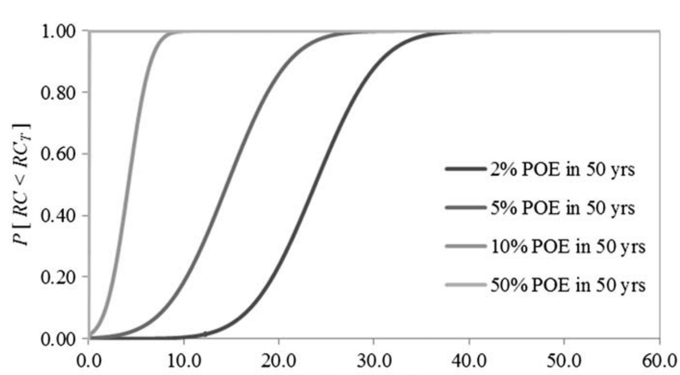

Figure 6. Distribution of losses for different hazard levels for a sample structure in Memphis.

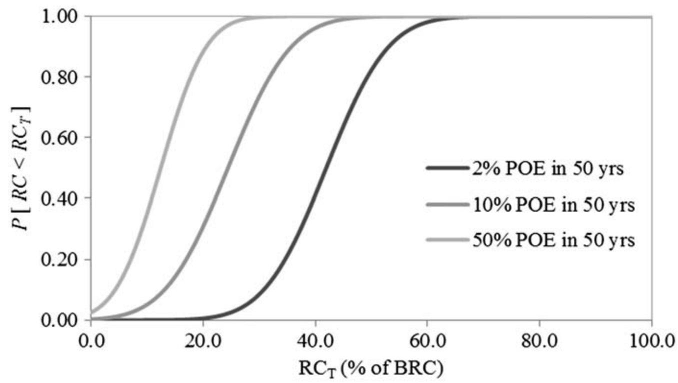

Figure 7. Distribution of losses for different hazard levels for a sample structure in Los Angeles.

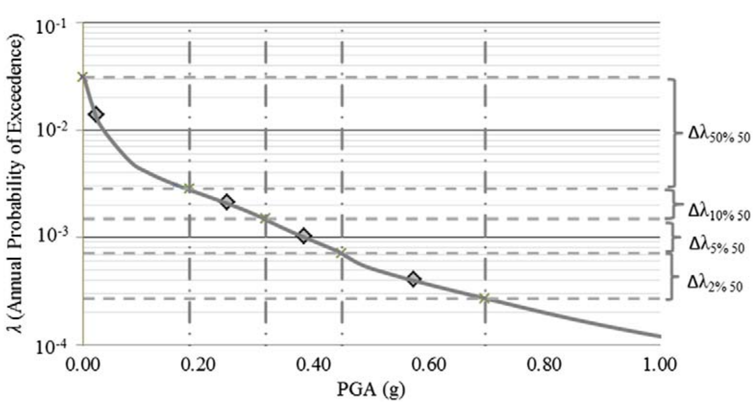

Figure 8. Memphis hazard curve, amplified for soil type D.

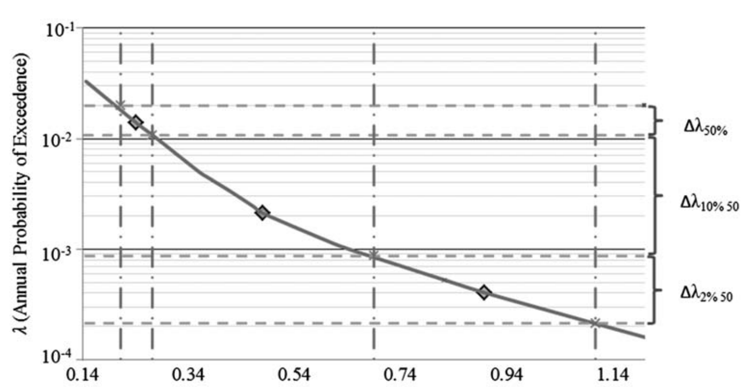

Figure 9. Los Angeles hazard curve, amplified for soil type D.

where $P[L > l]/yr$ is the annual probability of loss L exceeding specific value l, λ is the annual rate of exceedance for each IM_i, m is the number of hazard levels considered, and $\Delta\lambda_i$ is calculated from dividing the hazard curve into m different segments. Figure 8 shows the hazard curve for the Memphis site; since four hazard levels are considered in the analysis, the curve is divided into four segments ($m = 4$). It should be noted that increasing the number of segments would increase the accuracy of the results but would also result in more computationally expensive procedure. The effect of increasing the number of segments in the resulted loss values is not evaluated in this study. The first step is to locate the points on the hazard curve that are associated with the considered hazard levels (in this case, 2%, 5%, 10%, and 50% POE in 50 years). These points are marked as diamonds in Figure 8. The second step is to set the boundaries of the segments so that the considered hazard levels (indicated by diamonds on the curve) are located at the midpoint of each segment. From the segment boundaries, values for each $\Delta\lambda_i$ are determined. Figure 9 shows the hazard curve for Los Angeles developed using the same procedure. The difference is that the hazard curve is divided into three segments ($m = 3$) for the three hazard levels (2%, 10%, and 50% POE in 50 years) considered for the Los Angeles site.

Figure 10 shows the calculated total loss curves for a sample structure located in Memphis and Los Angeles. This curve is defined as the annual rate of exceeding for values of total loss represented as total repair cost (RC_T). The EAL parameter is calculated as the area under the total loss curve.

CALCULATION OF CONFIDENCE LEVELS

Confidence levels are calculated using the procedure presented in FEMA (2000a) and express the level of confidence in the structure's ability to meet the performance objectives. Confidence level CL is calculated as:

$$CL = \Phi(K_x) \tag{14}$$

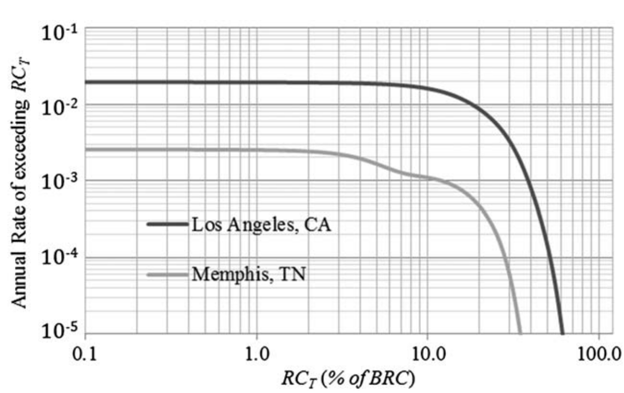

Figure 10. Total loss curve calculated for a sample structure located in Memphis and Los Angeles.

where $\Phi(K_x)$ is the normal cumulative distribution function value corresponding to K_x which is a standard Gaussian variant associated with probability x of not being exceeded (FEMA 2000a) and is calculated as:

$$K_x = \frac{k\beta_{UT}}{2} - \frac{\ln(\lambda_{CL})}{b\beta_{UT}} \tag{15}$$

where β_{UT} is an uncertainty measure equal to the vector sum of the logarithmic standard deviation of the variations in demand and capacity resulting from uncertainty (FEMA 2000a), b is a coefficient relating the incremental change in demand (ISDs and column forces) to an incremental change in ground shaking intensity at each hazard level, taken as 1.0 (FEMA 2000a), and k is the slope of the hazard curve, in natural log coordinates, at the hazard level of interest as calculated in FEMA (2000a). The confidence parameter λ_{CL} is calculated as the factored-demand-to-capacity ratio as:

$$\lambda_{CL} = \frac{\gamma\gamma_a D}{\phi C} \tag{16}$$

where γ is the demand variability factor accounting for the uncertainty inherent in the prediction of the ground motions; γ_a is an analysis uncertainty factor considering the uncertainty in the analytical procedure used to determine demand as a function of ground motion intensity; D is the calculated demand on a structure (obtained from a structural analysis); C is the median estimate of the capacity of the structure considered as ISD capacity and column compressive force capacity; and ϕ is a resistance factor that accounts for the uncertainty in the prediction of structural capacity. Values for these parameters are the recommended values by FEMA (2000a). Two performance objectives are selected: collapse prevention for hazard level of 2% POE in 50 years and immediate occupancy for hazard level of 50% POE in 50 years. Structural demands for the earthquake ground motions associated with selected hazard levels are determined and the nonlinear dynamic structural analysis is used to estimate the maximum ISD and maximum column compressive demand for the ground motions.

EXAMPLE STRUCTURAL DESIGN

Figures 11 and 12 show the geometry of the example structure adopted from SAC project (FEMA 2000b). The structural steel is A992 Grade 50-ksi. The lumped masses are calculated based on the loading presented in FEMA (2000b) for this structure. Based on these loading definitions, the seismic mass for the structure is calculated as 70.90 kips-sec^2/ft for roof and 65.53 kips-sec^2/ft for floors (the values are for the entire structure). Masses are lumped (LM_i) at the beam-to-column locations. Moment frame A-E is considered for the design. Lean-on columns are used in the analysis to represents the gravity frame system that is tributary to the moment resisting frame. In this example, since there are two moment resisting frames in the considered direction, the tributary gravity load associated with one half of the structure is assigned to the moment frame A-E/1.

Figure 12 shows the five design variables considered for the seismic PBD optimization (two column types C1 and C2 and three beam types B1, B2, and B3). The search space includes a list of 60 AISC W sections (W10, W12, and W14) for columns and another

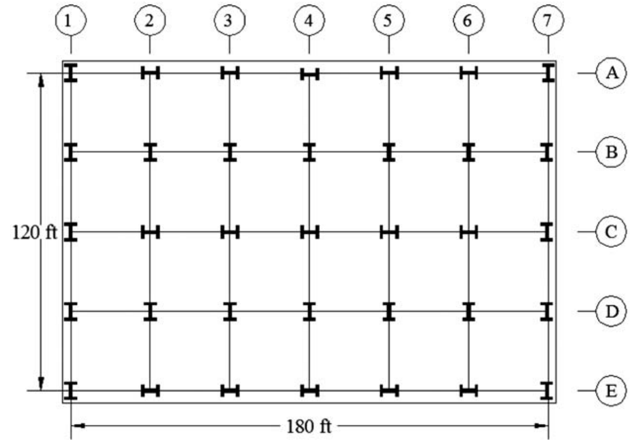

Figure 11. Plan layout of the example three-story structure.

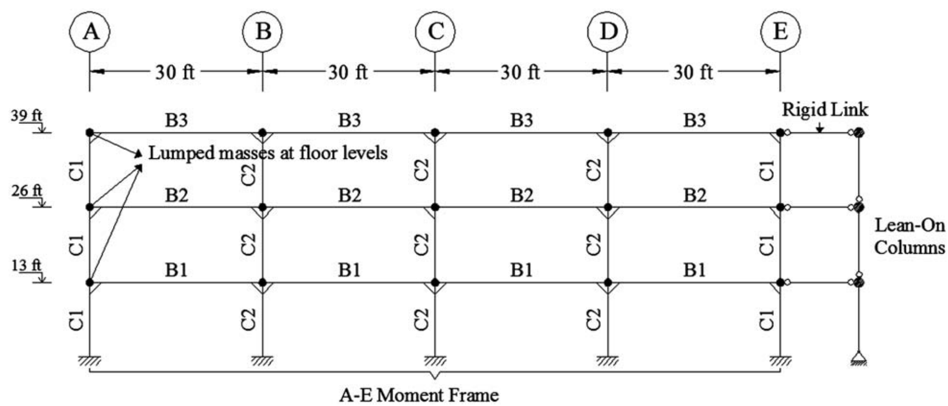

Figure 12. Elevation of the example three-story structure and considered design variables.

list of 64 AISC W sections (W18, W21, W24, W27, W30, W33, W36, and W40) for beam elements. The genetic algorithm uses a population size of 100, maximum number of generations of 300, a roulette wheel selection method, a uniform crossover method with probability of 0.6, and a mutation probability of 0.03. Figure 13 shows the Pareto front obtained using the NSGA-II multi-objective optimization strategy (Deb et al. 2002) for the combination of structural weight and EAL. The Pareto fronts represent a range of feasible designs that are mathematically equivalent. Table 2 lists the design details for the example frame for three sample designs located on the Pareto front for both geographic locations; design associated with the minimum weight, one design located on the middle of the front (which could be approximated as assigning similar importance to both optimization objectives), and design associated with the minimum EAL.

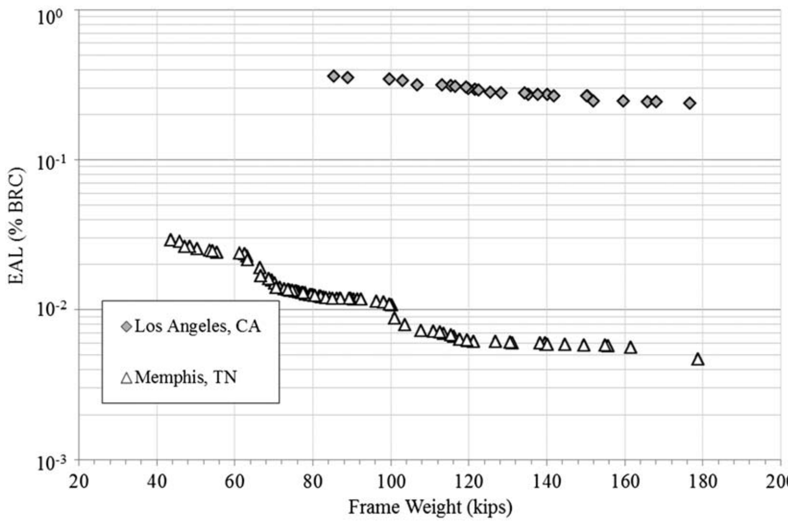

Figure 13. Pareto fronts for sites located in Memphis and Los Angeles.

Figures 10 and 13 show that values for EAL are significantly larger for a site located in Los Angeles compared to the site located in Memphis; the difference is associated with the seismicity characteristics of the two geographic locations characterized by the hazard curves. Comparing Figures 8 and 9 shows that for frequent earthquakes, associated with larger values of λ, the PGA values are larger on the Los Angeles hazard curve; the difference is less notable for rare events (smaller λ values). In addition, the slope of the hazard curve for Los Angeles is greater than that for Memphis, which could be attributed to the considerable difference in the calculated EAL values for these two locations. The ratio of the change in EAL to the change in weight, computed from Figure 13, is several times greater in Los Angeles than in Memphis, indicating an increase in weight would result in a significantly larger decrease

Table 2. Comparison of the results for the example frame located in Memphis and Los Angeles

Memphis, TN							
Designs	C1	C2	B1	B2	B3	W (kips)	EAL(%BRC)
Min Weight	W14X159	W14X109	W18X60	W21X50	W21X44	43.70	0.0291
Midpoint front	W14X257	W14X233	W30X99	W30X108	W30X124	87.16	0.0118
Min EAL	W14X550	W14X605	W33X201	W40X167	W36X170	178.82	0.0046
Los Angeles, CA							
Designs	C1	C2	B1	B2	B3	W (kips)	EAL(%BRC)
Min Weight	W14X342	W14X233	W21X93	W30X99	W24X68	85.41	0.3603
Midpoint front	W14X342	W14X426	W30X108	W33X141	W30X124	121.55	0.2931
Min EAL	W14X605	W14X605	W36X182	W36X150	W33X152	176.69	0.2383

in EAL. Using the Pareto fronts, decision makers would have a wider range of EAL to choose from for a structure in Los Angeles.

To compare the impact of seismic loss to the cost of the building, the present value of the total cost PC_t^T considering initial cost and seismic economic loss for a lifetime period of t years, is estimated as:

$$PC_t^T = C^I + PL_t^S \tag{17}$$

where C^I is the initial cost and PL_t^S is the present value of the seismic direct economic loss. The initial cost C^I is:

$$C^I = \rho \times W + C^0 \tag{18}$$

where ρ is the cost per unit weight of the frame and C^0 is the cost associated with components that are not a function of the W, such as the cost of the nonstructural components. Present value of the seismic economic loss PL_t^S is calculated as

$$PL_t^S = EAL \times \frac{(1 - e^{-it})}{i} \tag{19}$$

where i is discount rate assumed to be 2% (Porter et al. 2004) and t is considered to be 50 years (Ramirez et al. 2012, Porter 2003). The value of EAL in Equation 19 is calculated by considering the building replacement cost (BRC) to be equal to C^I. In the presented example, cost parameters are calculated for the specified frame and the constant parameter C^0 is excluded in the calculation of the PC_t^T. Table 3 lists the calculated ratios C^I/PC_{50}^T and PL_{50}^S/PC_{50}^T for the designs provided in Table 2. The ratio of seismic cost to the total cost of the structure is significantly higher in Los Angeles than in Memphis.

Figures 14 and 15 show the distribution of losses for selected designs. By moving from lighter structures to heavier structures with smaller EAL, the contribution of structural and drift-sensitive nonstructural components to the total loss value decreases and the contribution

Table 3. Costs for the example frame located in Memphis and Los Angeles

			Memphis, TN			
Designs	W (kips)	EAL (%BRC)	CL_{CP} (%)	CL_{IO} (%)	C^I/PC_{50}^T	PL_{50}^S/PC_{50}^T
Min Weight	43.70	0.0291	99.649	100.000	0.9909	0.0091
Midpoint front	87.16	0.0118	100.000	100.000	0.9963	0.0037
Min EAL	178.82	0.0046	100.000	100.000	0.9985	0.0015
			Los Angeles, CA			
Designs	W (kips)	EAL (%BRC)	CL_{CP} (%)	CL_{IO} (%)	C^I/PC_{50}^T	PL_{50}^S/PC_{50}^T
Min Weight	85.41	0.3603	92.422	51.991	0.8978	0.1022
Midpoint front	121.55	0.2931	99.812	99.997	0.9152	0.0848
Min EAL	176.69	0.2383	100.000	100.000	0.9300	0.0700

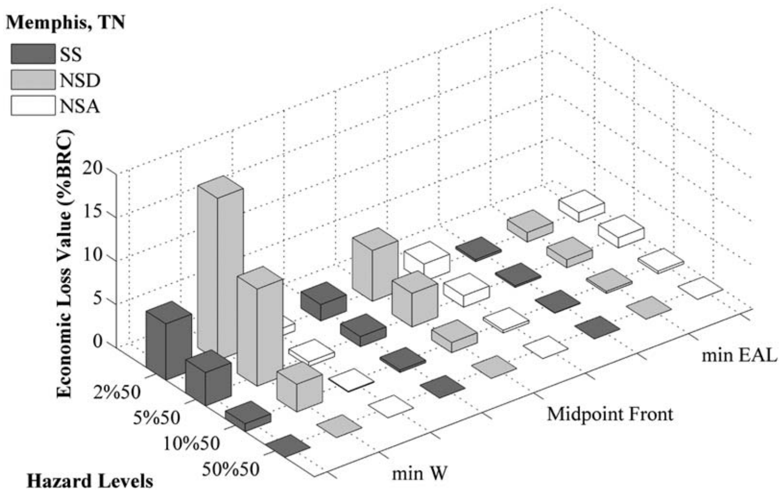

Figure 14. Distribution of losses for structures for Memphis.

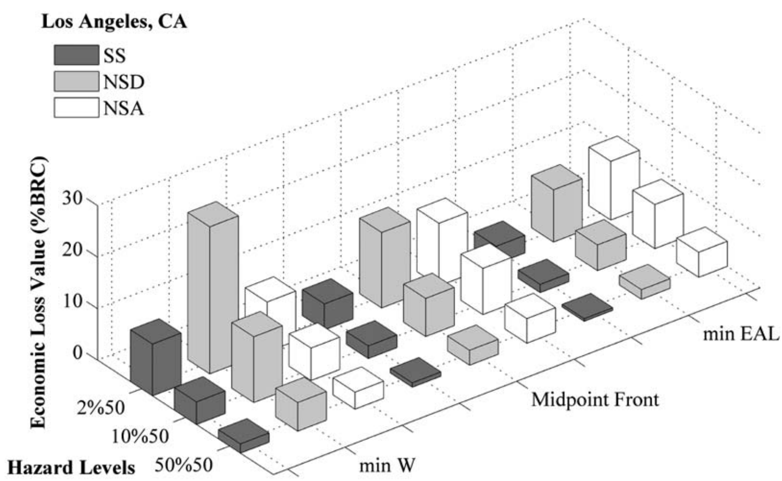

Figure 15. Distribution of losses for structures for Los Angeles.

of acceleration sensitive nonstructural components increases. Drift-sensitive nonstructural components have the highest contribution to the calculated seismic loss for all hazard levels for the three selected designs in Memphis and for the minimum weight and middle front designs in Los Angeles.

SUMMARY AND CONCLUSIONS

In this study, the expected annual loss (EAL) and the initial construction cost (the weight of the structure) are the optimization objectives for the PBD of structures. The obtained PBD

Pareto fronts provide engineers with a decision making tool for designing structures considering both initial cost and EAL. Additionally, effect of geographical location on the calculated loss values are evaluated by considering two different site locations: Memphis and Los Angeles. Seismic PBD results show a significantly larger seismic loss for structures located in Los Angeles than in Memphis, which are due to the differences in seismicity characteristics and slopes of the hazard curves in these locations. Consequently, for structures in Los Angeles, seismic loss should have a much greater role in real-state decision-making processes, as compared to structures in Memphis. Moreover, analyzing the distribution of losses indicates that in general, NSD components have the highest contribution to the total seismic loss associated with direct economic losses for most designs in both geographic locations. Additionally, by moving along the Pareto front from lower weight designs to higher weight designs, the contribution of structural (SS) and drift-sensitive nonstructural (NSD) components to total loss decreases and contribution of acceleration-sensitive nonstructural (NSA) components increases.

REFERENCES

Alimoradi, A., 2004. Probabilistic Performance-Based Seismic Design of Nonlinear Steel Structures Using Genetic Algorithm, Ph.D. Dissertation, University of Memphis.

Alimoradi, A., Pezeshk, S., and Foley, C., 2007. Probabilistic performance-based optimal design of steel moment-resisting frames. II: Applications, *Journal of Structural Engineering*, ASCE, DOI: 10.1061/(ASCE)0733-9445(2007)133:6(767).

American Association of State Highway and Transportation Officials (AASHTO), 2009. *AASHTO Guide Specifications for LRFD Seismic Bridge Design*, Washington, D.C.

American Institute of Steel Construction (AISC), 2011. *Seismic Design Manual, Second Edition*, Chicago, IL.

American Society for Testing and Material (ASTM), 2007. *Standard Guide for Seismic Risk Assessment of Buildings, E2026-07*, Torrance, CA.

Applied Technology Council (ATC), 2007. *Guidelines for Seismic Performance Assessment of Buildings*, ATC-58 35% Draft, Redwood City, CA.

Augusti, G., and Ciampoli, M., 2008. Performance-based design in risk assessment and reduction, *Probabilistic Engineering Mechanics* **23**, 496–508.

Bachman, R. E., 2004. The ATC-58 Project plan for nonstructural components, in *PEER Report 2004/05, Performance-Based Seismic Design Concepts and Implementation Proceedings of the International Workshop*, Bled, Slovenia, 28 June–1 July 2004, 125–136.

Baker, J. W., 2008. An Introduction to Probabilistic Seismic Hazard Analysis (PSHA), available at https://web.stanford.edu/~bakerjw/Publications/Baker_(2008)_Intro_to_PSHA_v1_3.pdf.

Bazeos, N., 2009. Comparison of three seismic design methods for plane steel frames, *Soil Dynamics and Earthquake Engineering* **29**, 553–562.

Beck, J. L., Irfanoglu, A., Papadimitriou, C., and Au, S. K., 2000. A performance-based optimal design methodology incorporating multiple criteria, in *12th World Conference on Earthquake Engineering*, Paper No. 314, Auckland, New Zealand.

Boore, D. M., 2000. SMSIM—Fortran Programs for Simulating Ground Motions from Earthquakes: Version 2.0—a Revision of OFR 96–80–A, available at http://geopubs.wr.usgs.gov/open-file/of00-509/.

Deb, K., Pratap, A., Agarwal, S., and Meyarivan, T., 2002. A fast and elitist multi-objective genetic algorithm: NSGA-II, *IEEE Transactions on Evolutionary Computation* **6**, 182–197.

Deierlein, G. G., 2004. Overview of a framework methodology for earthquake performance assessment. performance-based seismic design: concepts and implementation, in *PEER Report 2004/05, Performance-Based Seismic Design Concepts and Implementation Proceedings of the International Workshop*, Bled, Slovenia, 28 June–1 July 2004, 15–26.

Electric Power Research Institute (EPRI), 1993. *Guidelines for Determining Design Basis Ground Motions, Volume 2: Appendices for Ground Motion Estimation*, TR-102293 Project 3302 Final Report, Palo Alto, CA.

Federal Emergency Management Agency (FEMA), 2000a. *Recommended Seismic Design Criteria for New Steel Moment-Frame Buildings, FEMA 350*, Washington, D.C.

Federal Emergency Management Agency (FEMA), 2000b. *State of the Art Report on Systems Performance of Steel Moment Frames Subject to Earthquake Ground Shaking, FEMA 355C*, Washington, D.C.

Federal Emergency Management Agency (FEMA), 2006. *Next-Generation Performance-Based Seismic Design Guidelines-Program Plan for New and Existing Buildings, FEMA-445*, Washington, D.C.

Federal Emergency Management Agency (FEMA), 2008. *HAZUS MH Estimated Annualized Earthquake Losses for the United States, FEMA 366*, Washington, D.C.

Federal Emergency Management Agency (FEMA), 2012. *Seismic Performance Assessment of Buildings, FEMA-P-58-1*, Washington, D.C.

Foley, C., Pezeshk, S., and Alimoradi, A., 2007. Probabilistic performance-based optimal design of steel moment-resisting frames. I: Formulation, *J. Struct. Eng.* **133**, 757–766.

Fragiadakis, M., Lagaros, N. D., and Papadrakakis, M., 2006. Performance-based multiobjective optimum design of steel structures considering life-cycle cost, *Struct Multidisc Optim* **32**, 1–11.

Gen, M., and Cheng, R., 2000. *Genetic Algorithms and Engineering Optimization*, Wiley-Interscience, Hoboken, NJ, 512 pp.

Ganzerli, S., Pantelides, C. P., and Reaveley, L. D., 2000. Performance-based design using structural optimization, *Earthquake Engineering and Structural Dynamics* **29**, 1677–1690.

Gencturk, B., and Elnashai, A. S., 2011. *Multi-Objective Optimal Seismic Design Of Buildings Using Advanced Engineering Materials*, Mid-America Earthquake (MAE) Center Report No. 11-01, University of Illinois at Urbana-Champaign.

Hamburger, R., Rojahn, C., Moehle, J., Bachman, R., Comartin, C., and Whittaker, A., 2004. The ATC-58 Project: Development of next-generation performance-based earthquake engineering design criteria for buildings, in *13th World Conference on Earthquake Engineering*, Paper No. 1819, Vancouver, BC, Canada.

Hazus-MH, 2003a. *Hazus-MH MR1 Technical and User's Manual*, Multi-hazard Loss Estimation Methodology, FEMA, Washington, D.C.

Hazus-MH, 2003b. Hazus-MH MR4 Technical Manual- Multi-hazard Loss Estimation Methodology, FEMA, Washington, D.C.

Krawinkler, H., 2005. *Van Nuys Hotel Building Testbed Report: Van Nuys Hotel Building Testbed Report*, PEER Report 2005/11, Pacific Earthquake Engineering Research Center, University of California, Berkeley.

Liu, M., Burns, S. A., and Wen, Y. K., 2005. Multiobjective optimization for performance-based seismic design of steel moment frame structures, *Earthquake Engineering & Structural Dynamics* **34**, 289–306.

Miranda, E., Aslani, H., and Taghavi, S., 2004. Assessment of seismic performance in terms of economic losses, in *PEER Report 2004/05, Performance-Based Seismic Design Concepts and Implementation Proceedings of the International Workshop*, Bled, Slovenia, 28 June–1 July 2004, 149–160.

Moehle, J., and Deierlein, G., 2004. A framework methodology for performance-based earthquake engineering, in *13th World Conference on Earthquake Engineering*, Vancouver, BC, Canada.

Powell, G. H., 1993. DRAIN-2DX, Element Description and user guide for element Type01, Type02, Type04, Type06, Type09, And Type15, version 1.10, Report No. UCB/SEMM-93/18, Department of Civil Engineering, University of California, Berkeley, 1993-12, 68 pp.

Porter, K. A., 2003. An overview of PEER's performance-based earthquake engineering methodology, in *Proceedings, Ninth International Conference on Applications of Statistics and Probability in Civil Engineering*, San Francisco, CA.

Porter, K. A., Beck, J. L., and Shaikhutdinov, R., 2004. Simplified estimation of economic seismic risk for buildings, *Earthquake Spectra* **20**, 1239–1263.

Prakash, V., Powel, G. H., and Campbell, S., 1993. DRAIN-2DX base program description and user guide, Report No. UCB/SEMM-93/17, Department of Civil Engineering, University of California, Berkeley.

Shahbazian, A., and Pezeshk, S., 2010. Improved velocity and displacement time histories in frequency-domain spectral-matching procedures, *Bulletin of the Seismological Society of America* **100**, 3213–3223.

Ramirez, C. M., Liel, A. B., Mitrani-Reiser, J., Haselton, C. B., Spear, A. D., Steiner, J., Deierlein, G. G., and Miranda, E., 2012. Expected earthquake damage and repair costs in reinforced concrete frame buildings, *Earthquake Engineering & Structural Dynamics* **41**, 1455–1475.

Rojas, H. A., 2008. Automating the Design of Steel Moment-Frames Using a Probabilistic Performance-Based Approach and Evolutionary Computation, Ph.D. Dissertation, Memphis State University, 124 pp.

Rojas, H. A., Foley, C., and Pezeshk, S., 2011. Risk-based seismic design for optimal structural and nonstructural system performance, *Earthquake Spectra* **27**, 857–880.

Romero, S., and Rix, G. J., 2001. Regional variations in near surface shear wave velocity in greater Memphis area, *Engineering Geology* **62**, 137–158.

Somerville, P. G., Smith, N. F., Graves, R. W., and Abrahamson, N. A., 1997. Modification of empirical strong ground motion attenuation relations to include the amplitude and duration effects of rupture directivity, *Seismological Research Letters* **68**, 199–222.

U.S. Geological Survey (USGS), 2008. Documentation for the 2008 Update of the United States National Seismic Hazard Maps, Open-File Report 2008-1128, Reston, VA.

Xu, L., Yanglin, G., and Grierson, D. E., 2006. Seismic design optimization of steel building frameworks, *Journal of Structural Engineering* **132**, 277–286.

(Received 5 August 2013; accepted 21 November 2015)